



Modeling the effects of land use/land cover changes on water requirements of Urmia Lake basin using CA-Markov and NETWAT models

Kiyoumars Roushangar^{1,2} · Mohammad Taghi Alami¹ · Hassan Golmohammadi¹

Received: 10 October 2022 / Accepted: 7 December 2022 / Published online: 27 December 2022
© The Author(s), under exclusive licence to Springer Nature Switzerland AG 2022

Abstract

Urmia Lake, the largest inland lake in Iran, is facing a severe drying scenario, with dire consequences for the whole region. The rapid expansion of agricultural activities in the Urmia Lake basin has predominately led to tremendous pressure on the limited water resources, which has accelerated the drying process of this lake. The objective of this study is to analyze the spatio-temporal dynamics of land use/land cover (LULC) (2000–2020) and simulate agricultural expansion (2030 and 2040) in the Urmia Lake basin. Support Vector Machine (SVM)-based classification approach was used on Landsat satellite imagery from 2000, 2010, and 2020 to derive respective LULC layers. Cellular Automata (CA)-Markov and Land Change Modeler (LCM) were employed to simulate and assess future agricultural growth and land cover changes. Furthermore, the water requirement of agricultural activities was estimated with the NETWAT model. The results showed that the areas covered by irrigated agriculture and gardens are projected to experience a significant increase. These findings indicated that the actual LULC change during 2000–2020 was 68,802 ha of garden growth (174% change), while the simulated change was expected to be 127,613 ha by 2040. Moreover, the statistical result showed an increase of irrigated and rain-fed agricultural lands by 147,948 ha (55.98%) and 356,372 ha (145.69%), respectively, by 2040. Adopting the NETWAT model, this study suggests that the changes in LULC of the region will increase the water requirement of agriculture activities from 1500 billion cubic meters in 2000 to more than 4100 billion cubic meters in 2040.

Keywords Land use/land cover change · Markov-cellular automata · Land change modeler · Support vector machine · Urmia Lake

Introduction

Threats caused by climate change and other global environmental changes are among the obstacles to human progress in achieving sustainable development goals. Rapid

urbanization, population growth, and other socio-economic development activities are the primary drivers in the emergence of such changes that cause deforestation and land cover alteration. Deforestation can lead to the loss of biodiversity and has destructive effects on the terrestrial and aquatic ecosystems of the planet (Wang et al. 2020). Being essential parts of environmental changes and the Land Use/Land Cover (LULC) change have considerable impacts on a region's hydrological cycle and agricultural systems (Calanca, 2007). The way the earth's surface is covered by wetlands, forests, agriculture, impermeable surfaces, and other types of land and water is expressed by the concept of land cover (Prakasam, 2010).

On the other hand, the way humans use the landscape for conservation, development, or mixed uses is also defined by the concept of land use. Land use consists of agricultural land, recreation areas, built-up areas, and wildlife habitats (Reis et al. 2008). The land use/land cover changes

✉ Kiyoumars Roushangar
Kroshangar@yahoo.com

Mohammad Taghi Alami
mtaalami@tabrizu.ac.ir

Hassan Golmohammadi
hassangm27326@gmail.com

¹ Department of Water Resources Engineering, Faculty of Civil Engineering, University of Tabriz, 29 Bahman Ave, Tabriz, Iran

² Center of Excellence in Hydroinformatics, University of Tabriz, Tabriz, Iran

significantly affect crop productivity due to the lack of freshwater availability (Nyatuame et al. 2020). Therefore, assessing the magnitude and pattern of land cover types is necessary to project the future of water resources and land development, especially for areas where the primary land cover is water-dependent (agricultural land). LULC covers studies of deforestation, agricultural expansion and intensification, the energy footprint, and urban growth (Montalván-Burbano et al. 2021).

There is a large volume of published studies confirming the critical role of agricultural expansion on the water balance of agricultural watersheds (Sahoo et al. (2018); de Hipt et al. (2019); Ni et al. (2021); Idrissou et al. (2022); Ougahi et al. (2022); Abungba et al. (2022). Among themes, Schilling et al. (2008) investigated the potential impacts of future LULC change on the annual and seasonal water balance of the Raccoon River watershed through the SWAT (Soil and Water Assessment Tools) model. The results show an increase in water yield and nitrate, phosphorus, and sediment losses with corn production.

Grecchi et al. (2014) assessed the changes in land use patterns of the Brazilian Cerrado and their impacts on the environment through a multidisciplinary approach. Their results revealed a drastic landscape change from vegetation to an integrated agricultural area, which caused a sharp increase in the risk of erosion in the region. Kumar et al. (2018), in their study on the Tons River Basin of India, found that LULC changes had significantly affected the water availability in this region, leading to a decrease in surface runoff and lateral flow from 62.29 and 2.39% to 2.39 to 62.14% and 0.261%, respectively. Aghsaei et al. (2020) applied SWAT to determine the effect of LULC change on the hydrological response of the Anzali wetland catchment in Iran. The results indicated that the increase in agricultural land use resulted in an increase of evapotranspiration, water yield, and sediment yield by up to 8.3, 7, and 169%, respectively. The study by Samal and Gedam (2021) showed that the nature of LULC change has differential impacts at both basin and sub-basin scales. At the basin level, the impact of LULC change on hydrological parameters is, however, at the sub-basin level, the surface runoff and water yield increase significantly.

Considerable efforts have been made to develop efficient methods for modeling and predicting land use change (Veldkamp and Lambin 2001; Overmars 2003). Markov chain analysis is one of the common models based on the stochastic modeling approach that has been widely used to investigate the dynamics of land use change and predict its trend in future (Mubea et al. 2011; Kumar et al. 2014). This model works based on a series of random values whose probability depends on past values. (Dadhich and Hanaoka 2010; Zhang et al. 2011). Furthermore, as a simple method, the Markov chain is a proper tool to predict all multidirectional land-use changes

and is utilized when the definition of the landscape changes is complex (Weng 2002; Pontius and Malanson 2005). Integrated modeling approaches such as integrated Markov chain and cellular automata (CA-Markov) are suggested to be more appropriate for modeling land use change procedures (Guan 2011). Therefore, the CA-Markov model has been used to simulate LULC changes in different regions of the world (Nouri et al. 2014; Mansour et al. 2020; Sibanda and Ahmed 2021; Fu et al. 2022; Weslati et al. 2022). Land Change Modeler (LCM) is another modern and commonly used model that has revolutionized the analysis of land cover conversions and predicting land use changes in future. Dynamic projection proficiency, proper calibration, and the ability to simulate several types of land cover are among the reasons for the expansion of the use of the LCM model (Abuelaish and Olmedo 2016; Shooshtarian et al. 2018; Hasan et al. 2020; Qacami et al. 2022; Hussien et al. 2022; Tariq et al. 2022).

Based on the above discussions, land use/land cover models provide social and economic benefits in making decisions and understanding the process of changes and future projections of a watershed. Changes. Iran has faced severe problems due to rapid urbanization and extensive land use changes as a developing country. Land use changes in Iran have accelerated in the last 50 years. Land use and land cover and subsequent destruction of water and forest resources are one of the main concerns in Iran's environmental issues. Urmia Lake, as one of Iran's most important natural ecosystems, the second largest saline lake in the world, has an important national and international position, which has undergone a dramatic decline in its water level. Climate change, human activities, and unbalanced development of agriculture in the catchment area are among the primary factors in decreasing the water level of the Urmia Lake, which have been debated in scientific literature. The literature review showed that the conducted studies have a particular focus on the effects of past land use change, and the effects of future land use changes on the catchment area of the Urmia Lake have not been investigated.

In most cases, prospective studies of Urmia Lake have addressed the effects of climate change. However, there is no comprehensive study concerning the effects of land use changes (especially agricultural land use) on the water requirements of the Urmia Lake basin. Therefore, the main goal of the present study is to use the CA-Markov model to simulate future land use changes in the Lake Urmia basin and investigate its effects on the agricultural water requirements of the region.

Materials and methods

Study area

Urmia Lake is located in the northwest of Iran, and with an area of $\sim 5700 \text{ km}^2$, it is considered the third largest saline lake worldwide. The lake watershed area is $\sim 52,000 \text{ km}^2$ and has an elevation range from 1256 to 3720 m.a.s.l. The basin of the lake is located between the provinces of West Azerbaijan (0.46), East Azerbaijan (0.43), and Kurdistan (0.10). The average water intake volume of the lake, which is situated at the height of 1274 m above sea level, is 32 billion m^3 . The most important sources of water supply in the Urmia Lake are rivers of the catchment basin and direct precipitation over its surface. Six rivers from the east, five from the west, and four from the south are the main rivers providing water to Lake Urmia. The ecosystem of the lake is a generally mountainous territory, including two of the well-known Iranian volcanic peaks (Sabalan, 4810 m, and Sahand, 3707 m), and with numerous

immense productive plains in the valleys and around the lake. The location of the study area is depicted in Fig. 1.

Data and software used

Selecting appropriate classified satellite images is the most important process in simulating the future land use map. The satellite imagery dataset used in the present study is composed of the Thematic Mapper (TM), Enhanced Thematic Mapper Plus (ETM+), and the Operational Land Imager (OLI) Landsat sensors on board Landsat 5, Landsat 7, and Landsat 8, respectively. Landsat satellite images were collected during different periods (2000–2010–2020) for the Urmia Lake basin from the United States Geological Survey (USGS) (<https://earthexplorer.usgs.gov>). The image information is provided in Table 1.

Pre-processing of images in the form of image enhancement, geometric, atmospheric, radiometric, and topographical corrections was carried out in the Envi software environment. The land use map was obtained through the Support Vector Machine (SVM) classification algorithm in the

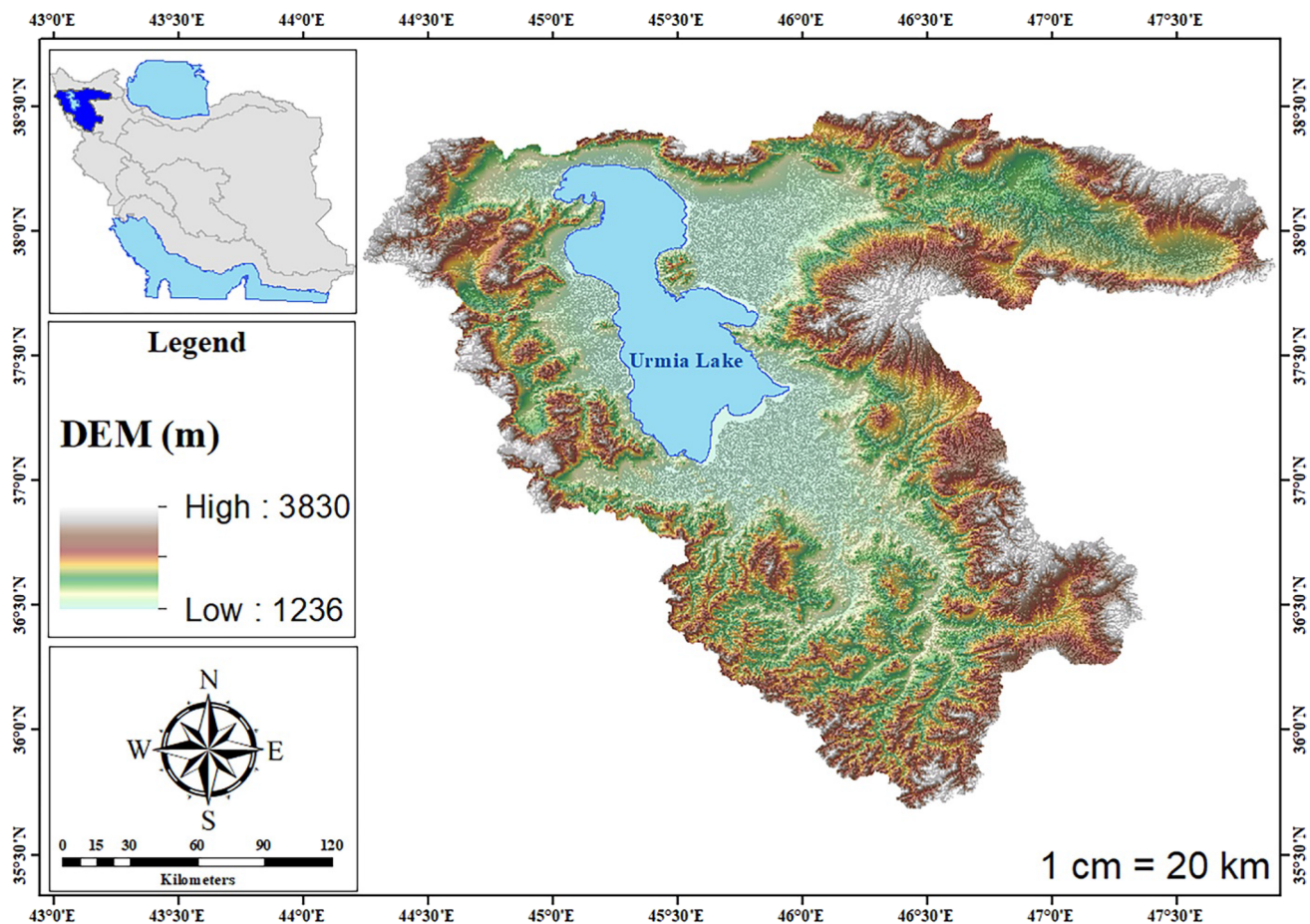


Fig. 1 The location of the study area

Table 1 Landsat image information

Satellite	Type	Path/row	Date	Resolution (m)
Landsat 5	TM	167:034–035	22/08/2000	30
		168:033–034-035		
		169–034-035		
Landsat 7	ETM+	167:034–035	22/08/2010	30
		168:033–034-035		
		169–034-035		
Landsat 8	OLI/TIRS	167:034–035	16/08/2020	30
		168:033–034-035		
		169–034-035		

desired period. The CA-Markov and Land Change Modeler (LCM) modules, which are all available within TerrSet, were used to predict possible land use changes for the years 2030 and 2040. Finally, the future water requirements of agricultural activities were calculated through the NETWAT model.

Support vector machine-based classification

SVM classifier has been developed by Cortes and Vapnik (1995) as a robust supervised classification technique for handling high-resolution multi-band images and extensive segmented satellite data. SVM provides an approach based on non-parametric learning, which causes insensitivity to data distribution (Fauvel et al. 2009). The SVM algorithm is based on creating an optimal hyper-plane in a high or infinite dimensional space by maximizing the spread between classes. Less sensitivity to noise, correlated bands, and the unbalanced number of training data are among the advantages of SVM compared to other classification algorithms (Cawley and Talbot 2010). In the classification process by SVM, the acceptable level of misclassification is determined by the penalty parameter. The penalty parameter permits control of the trade-off between “allowing training errors” and “enforcing strict margins. It is possible to achieve a more accurate model in the SVM method by increasing the penalty parameter and thus reducing the number of misclassified pixels. The training sets are projected from the input space to another higher dimensional feature space by the kernel function so that a linearly separable output dataset is obtained. In the present study, Radial Basis Function (RBF) kernel is used as a core tool of employed SVM technique in the classification process as formulated below (Yang et al. 2008; Singh et al. 2014):

$$k(x_i, x_j) = \exp(-\gamma \|x_i - x_j\|^2) \quad (1)$$

where x_i and x_j are vectors in the input space, respectively.

Image classification accuracy

Accuracy assessment of classification for land-use patterns can help determine the applicability of selected machine learning algorithms in land-use planning. Ground truth data was used to evaluate the accuracy of classified maps. For 2000 and 2010, the reference points were collected from Google Earth, and for the 2020 image, the ground truth data obtained from the original land-use map and field observation was used. In this work, the kappa coefficient was used to assess the classification accuracy:

$$\frac{N \sum_{i=1}^r x_{ii} - \sum_{i=1}^r (x_{i+})(x_{+i})}{N^2 - \sum_{i=1}^r (x_{i+})(x_{+i})} \quad (2)$$

where r represents the number of rows in the matrix, x is the number of observations in row i and column i (the diagonal elements), x_{i+} and x_{+i} are the marginal totals of row r and column i , respectively, and N is the total number of observations.

CA-MARKOV model

CA-Markov model is a combined Cellular Automata/Markov chain land prediction model that supposes a component of spatial contiguity and knowledge of the likely spatial distribution of transitions to Markov chain analysis. In the proposed integrated model, the Markov chain model, as a discrete-time stochastic model, simulates the LULC change probabilities through a transition probability matrix (Eastman 2006; Mishra et al. 2011). In the next step, the transition trend between different LULC states is determined using the transition probability among two states of t_1 and t_2 (Wu et al. 2010; Mosammam et al. 2017). The Markov chain model provides an appropriate estimate of the magnitude of LULC occurrences but cannot provide the spatial distribution of these changes (Yang et al. 2012; Maviza and Ahmed 2020). However, Cellular automata (CA), can change and control complex spatially distributed processes, with a strong ability to simulate the spatio-temporal characteristics of complex systems (Guan et al. 2011a, b). The CA model can be formulated as follows (Sang et al. 2011):

$$S(t, t+1) = f(S(t), N) \quad (3)$$

where S is the set of limited and discrete cellular states, N indicates the Cellular field, t and $t+1$ represent the different times, and f is the transformation rule of cellular states in local space. The Markov model is a theory based on the formation process of Markov random process systems for the prediction and optimal control theory method. Calculation of the land use changes prediction in accordance with the conditional probability formula—Bayes can be expressed as follows (Memarian et al. 2012; Ma et al. 2012):

$$S(t + 1) = P_{ij} \times S(t) \tag{4}$$

where $S(t)$ and $S(t + 1)$ stand as the system status at the time of t and $t + 1$, respectively; P_{ij} stands as the transition probability matrix in a state, which is calculated as follows:

$$P = (P_{ij}) = \begin{pmatrix} P_{11} & P_{12} & \dots & P_{1n} \\ P_{21} & P_{22} & \dots & P_{2n} \\ \dots & \dots & \dots & \dots \\ P_{n1} & P_{n2} & \dots & P_{nn} \end{pmatrix}, \sum_{j=1}^n P_{ij}=1 \tag{5}$$

where P is the Markov transition matrix, P_{ij} is the probability from LULC type i to land type j , and n is the number of LULC types in the study area. The transition matrix requests that each rate is a non-negative quantity and each line factor 0 to 1. The relative frequency of the transition observed during the whole period is considered an estimate of the Markov chain. The result of the estimation can be used for prediction.

Land change modeler

The LCM (Land Change Modeler) embedded in the TerrSet Geospatial Monitoring software was utilized to predict the future LULC for a particular year relying on the classified historical satellite images. The LCM is a land change prediction tool for land planning that is very popular due to its simplicity, graphical illustration, and availability of different modeling approaches (Eastman and Toledano 2018). The LCM module allows Multi-Layer Perceptron (MLP) neural network, logistic regression, and Multi-Objective Land Allocation (MOLA) to generate maps of transition potential based on the individual sub-models and associated explanatory variables. LCM uses historical LULC maps to empirically model the relationship between land cover transitions and descriptive variables to map future LULC scenarios. The prediction of future land cover in LCM consists of four main steps: (1) analyzing historical changes in land cover, (2) generating transition matrix maps, (3) validating the model, and (4) predicting the future land cover map.

NETWAT model

Known as the national document, the NETWAT model determines the demands and needs for farming and horticultural plants. The NETWAT model has been developed for the use of agricultural water consumption optimization committees in the provinces of Iran. This software provides data on the transpiration and evaporation of plants grown in 620 fields in Iran. With a correct estimation of such evaporation and transpiration, it is possible to effectively manage these farming and horticultural practices (Goodarzi et al. 2022). The NETWAT model includes the meteorological data for a

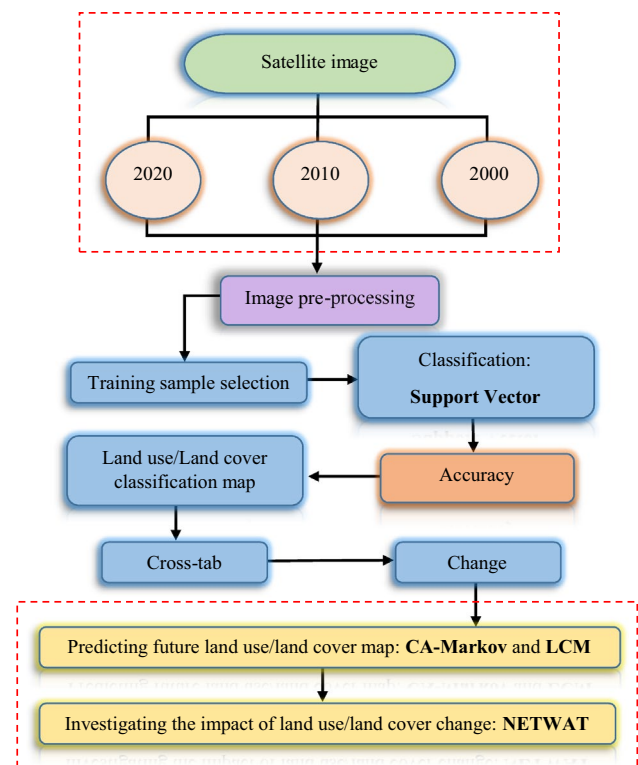


Fig. 2 An overview of detecting and predicting land-use changes in the Urmia Lake basin

reformed period of 60 years. The Penman–Monteith method of FAO is the basis of the calculation model of this software (Hosseini Baghanam et al., 2022). The output of the NETWAT model as Iran’s national water document is the project “Iran’s pure water requirement of crops and garden products,” carried out by Iran’s Ministry of Agriculture and Iran Meteorological Organization (IMO). The steps of the modeling process in the present study is illustrated in Fig. 2.

Results and discussion

LULC variation

The land use land cover maps offer a deeper understanding of land use change trends. The results indicate the history of land use change and the change quantity in each LULC class. Figure 3 illustrates three LULC maps of the whole Urmia Lake watershed generated by the SVM for the years 2000, 2010, and 2020. The overall accuracy of the maps assessed with 100 reference points per land-cover class was more than 84% and produced kappa indices over 0.84 (Table 2). The types of land use/cover were classified into nine categories, which include water, irrigated agriculture, rain-fed agriculture, sandy areas, rocky areas, salty areas, rangeland

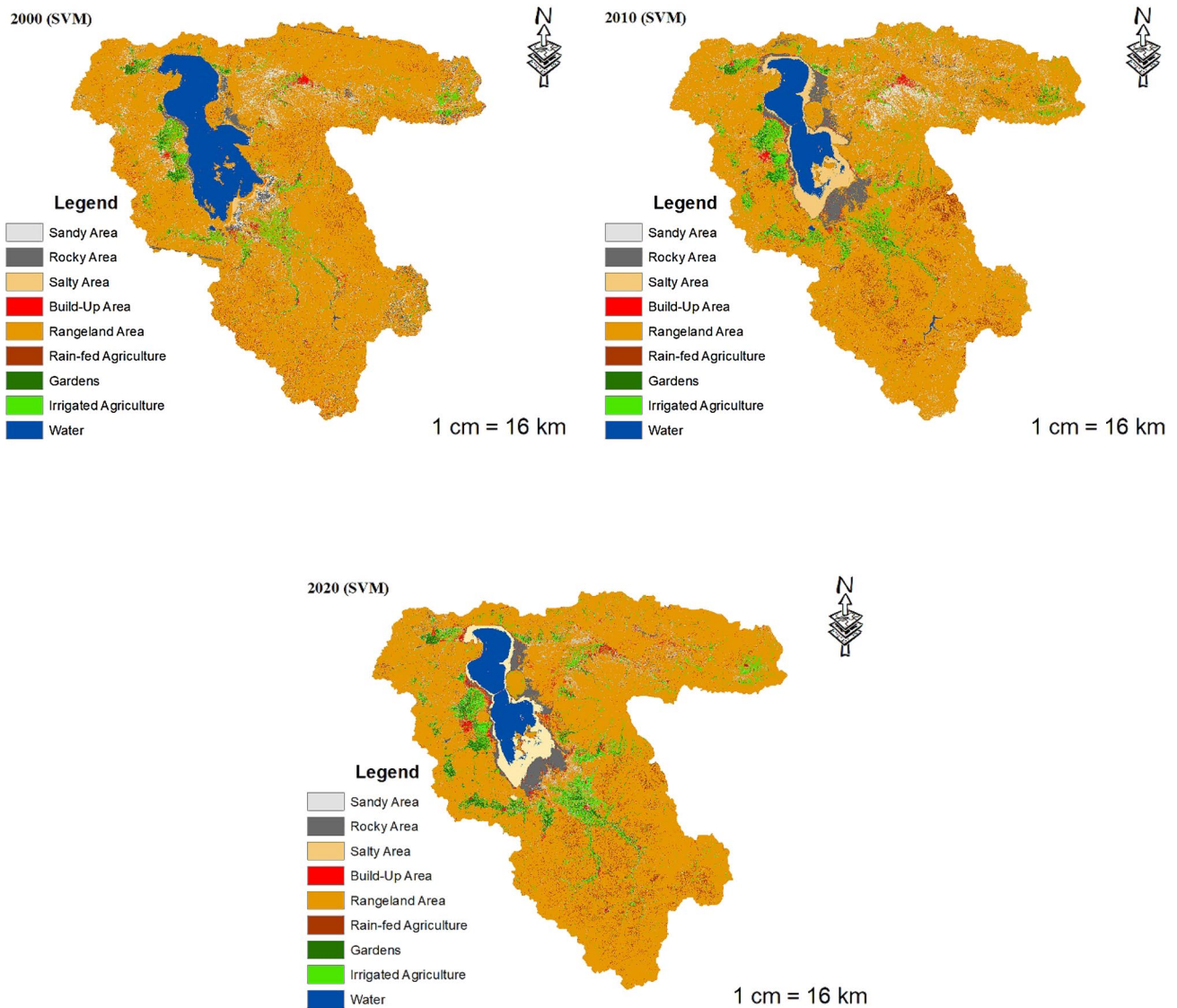


Fig. 3 Land use and land cover change (LULC) change map of the Urmia Lake catchment area in three different stages 2000, 2010 and 2020

areas, built-up areas, and gardens. In three classification maps, the rangeland area is the dominant LULC type of the Urmia Lake watershed which covered 78% of the study area in 2000, 75% in 2010, and 76% in 2020. The sandy areas, which represent the sandy plain, cover most of the southern part of Urmia Lake. The remaining LULC classes cover only about ~17% (2000) to 21% (2020) of the landscape.

The results of land-use changes for the years from 2000 to 2020 are summarized in Fig. 4. From 2000 to 2020, gardens increased by 174% (108,328 ha), irrigated agriculture by 86% (270,350 ha), and rain-fed agriculture by 38% (131,557 ha). Built-up areas including residential areas, roads, and other types of built-up areas, occupied only about 1% of the landscape in the first stage (represented by the 2000 map). The development of the regional economy and

the growth of the population in the city has caused an 82% increase in built-up areas in the third stage (represented by the 2020 map). On the other hand, the reduction of the lake water area by 53% (221,347 ha) has caused a significant increase in the salty areas by 779% (149,315 ha).

Assessment of future LULC variation through the CA–Markov model

In subsequent, CA-Markov was employed for predicting the LULC changes according to historical data from 2000, 2010, and 2020. Furthermore, the LCM model was used for comparative purposes. For this purpose, after examining the results of the spatial accuracy of the land-use changes modeling in the base years, the CA–Markov model was used

Table 2 Overall accuracy and kappa index of the agreement for LULC classification for 2000, 2010, and 2020

Land use	Year		
	2000	2010	2020
Sandy areas	82.2%	90.2%	92.8%
Rocky areas	81.5%	78.9%	95.4%
Salty areas	80.9%	98.3%	100%
Built-up areas	80%	77.1%	96.1%
Rangeland areas	82.4%	89.1%	91.8%
Rain-fed agriculture	92.9%	73.9%	95.6%
Gardens	87.8%	90.3%	95.2%
Irrigated agriculture	95.4%	90.2%	93.7%
Water	92.1%	94.7%	93.8%
Kappa	0.848	0.872	0.924
Overall accuracy	87.78%	84.39%	94.71%

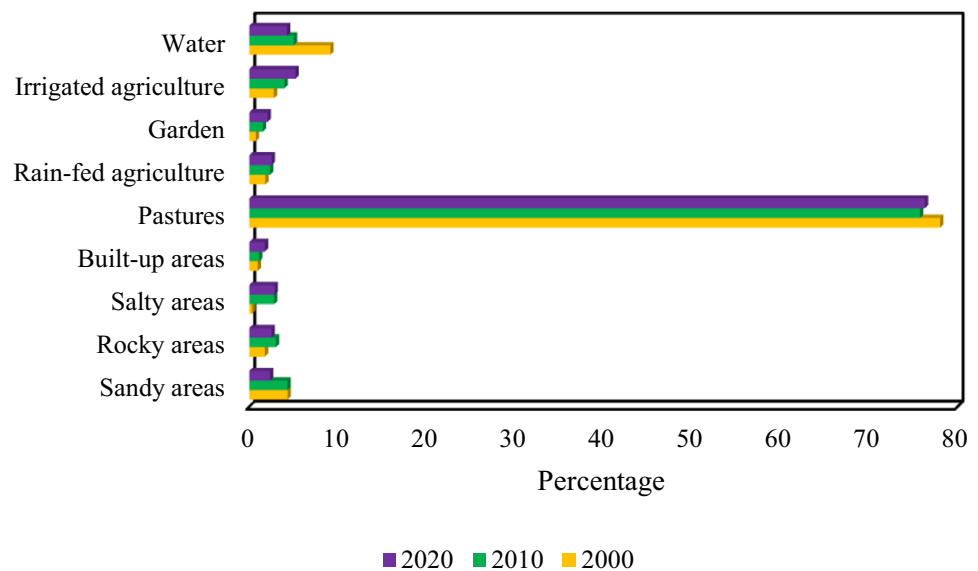
to predict the land-use changes until the years 2030 and 2040. Figure 5 demonstrates the predicted land-use map for 2030 and 2040 through CA-Markov and LCM models. The prediction of the potential distribution of the LULC classes in 2030 and 2040 demonstrates significant growth in gardens. It also shows expansion in irrigated agriculture and rain-fed agriculture. The considerable changes in landscape development can be distinguished over the entire period from 2000 to 2040 from the CA-Markov and LCM models. The results obtained from the CA-Markov model show that irrigated agriculture land will increase from 1450 km^2 (2000) to more than 3200 km^2 (2030) and 3500 km^2 (2040). Gardens will increase by about 240% in 2030 (1350 km^2) and 323% in 2040 (1671 km^2) compared with 2000 (395 km^2). At the same time, the area covered by rain-fed agriculture will increase from 498 km^2 in 2000 to 1430 km^2

in 2030, and 1470 km^2 in 2040. This increase in these areas reflects the Iranian government's policy for economic development through increasing agricultural production, which started at least two decades ago. The deterioration of natural land cover is one of the consequences of the current trend of land use change.

Most importantly, the pressure on underground water resources in these areas will increase, and as a result, it will cause subsidence in the plains. Moreover, in the absence of legal considerations, these changes cause unsustainable water withdrawal, which has caused a decrease in the level of the Urmia Lake by influencing the inflow. Similar to the CA-Markov model and based on the outputs of the LCM model, it is expected that the LULC classes in the Urmia Lake catchment area will continue to change. The prediction results of the LCM model in the year 2030 show a maximum difference of 3% with CA-Markov. Meanwhile, the difference between the predictions of LCM and CA-Markov will reach 5.7% in 2040.

Summaries of the probability matrix between LULC classes during the periods 2020–2030 and 2020–2040 were listed in Tables 3 and 4. Row categories in Table 3 describe LULC classes in 2000, and column categories describe classes of 2030. The Rangeland areas had a probability as high as 62.9% to remain as rangeland in 2030. Rocky areas also had a probability as high as 67.53% to remain as rocky areas in 2030. Gardens and built-up areas were a lesser amount probability of 39.7 and 32.53%, respectively, to remain as they are. The most striking conclusion to emerge from the results of the Tables 3 and 4 is that the probability of change in irrigated agriculture to gardens is 25.03%, and this coefficient will reach more than 36% in 2040.

Fig. 4 Land use and land cover change (LULC) change of the Urmia Lake catchment area



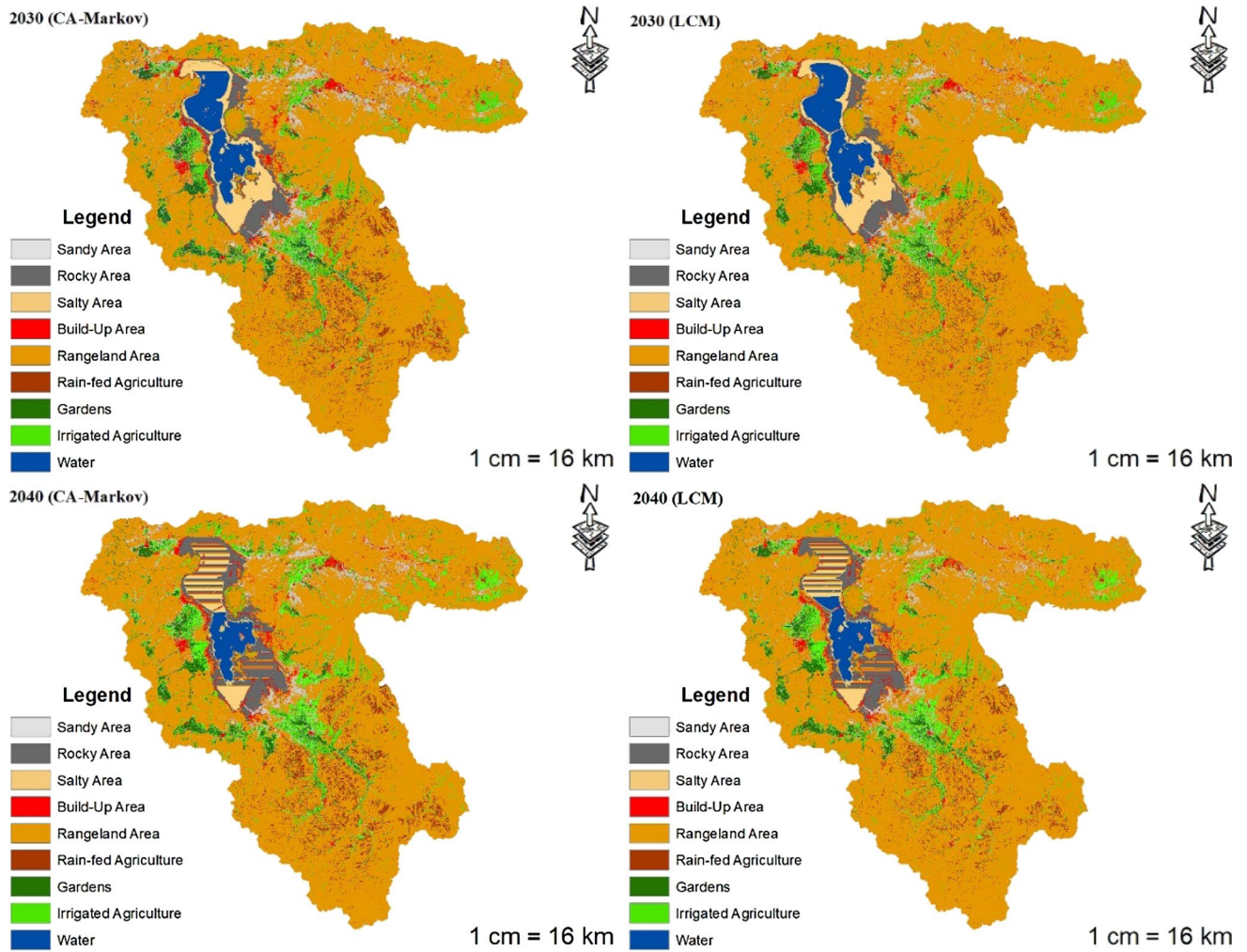


Fig. 5 The predicted 2030 and 2040 LULC of the Urmia Lake watershed

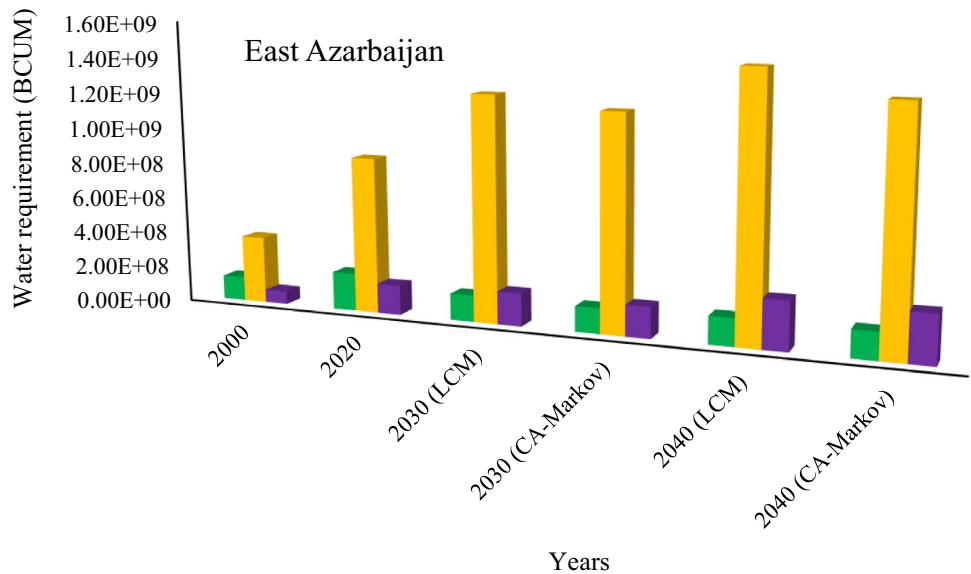
Table 3 Transition probability matrix of LULC during 2020–2030

Land use and cover in 2020	Land use and cover in 2030								
	Sandy areas	Rocky areas	Salty areas	Built-up areas	Rangeland areas	Rain-fed agriculture	Gardens	Irrigated agriculture	Water
Sandy areas	0.0667	0.0158	0.0039	0.0362	0.8549	0.0015	0.0034	0.0176	0
Rocky areas	0.0582	0.4333	0.0117	0.112	0.3805	0.00211	0.0003	0.0017	0.0001
Salty areas	0.0023	0.1848	0.6753	0.028	0.0409	0.0011	0.0004	0.0017	0.0655
Built-up areas	0.0804	0.1189	0.0011	0.3253	0.439	0.0023	0.0085	0.0244	0.0001
Rangeland areas	0.0791	0.0318	0.0029	0.0425	0.629	0.091	0.0172	1.1061	0.0003
Rain-fed agriculture	0.0037	0.0003	0	0.0008	0.8228	0.1375	0.0068	0.0281	0
Gardens	0.022	0.0001	0	0.0024	0.1341	0.0054	0.397	0.4389	0
Irrigated agriculture	0.0589	0.0003	0.0001	0.0081	0.2839	0.0037	0.2503	0.3947	0
Water	0.0017	0.0008	0.2343	0.0034	0.0425	0	0	0.0003	0.717

Table 4 Transition probability matrix of LULC during 2020–2040

Land use and cover in 2020	Land use and cover in 2040								
	Sandy areas	Rocky areas	Salty areas	Built-up areas	Rangeland areas	Rain-fed agriculture	Gardens	Irrigated agriculture	Water
Sandy areas	0.1155	0.0347	0.0005	0.0556	0.7305	0.0097	0.008	0.0443	0.0004
Rocky areas	0.0917	0.1671	0.0022	0.1418	0.5683	0.0084	0.0034	0.017	0
Salty areas	0.017	0.6321	0.0007	0.0633	0.2755	0.0075	0.0001	0.0037	0
Built-up areas	0.0463	0.0226	0.0003	0.1215	0.6621	0.0029	0.0256	0.1185	0.0001
Rangeland areas	0.0466	0.0249	0.0024	0.027	0.7184	0.071	0.0257	0.0838	0.0002
Rain-fed agriculture	0.0097	0.0007	0	0.0073	0.9261	0.0088	0.0103	0.0371	0.0001
Gardens	0.0206	0.0005	0.0001	0.0077	0.1258	0.0011	0.4766	0.03641	0.0036
Irrigated agriculture	0.0517	0.0004	0.0001	0.0147	0.2486	0.0051	0.2199	0.4585	0.001
Water	0.0013	0.1391	0.3169	0.0188	0.0821	0.0007	0.0002	0.001	0.4398

Fig. 6 Water requirement of the sub-basin of East Azarbaijan Province for agriculture in the period of 2030–2040



Assessment of future water requirements through the NETWAT model

Expansion of cropland and gardens in the region requires more water withdrawal and affects the water resources. Therefore, in the next stage of this research, the amount of water requirements for each product in each province and plain for the future of the Urmia Lake watershed was calculated using the NETWAT model. As mentioned previously, the NETWAT model, which was developed based on Iran’s National Water Resources Development Plan, contains information related to a variety of crops produced in 620 plains of Iran and has been optimized according to the climatic and

soil conditions of Iran’s plains. Assessing the outcomes of the NETWAT model for the future water resource requirements of agriculture in the sub-basin of East Azarbaijan province, it showed that the increase in the area covered by agriculture activities, especially gardens and irrigated agriculture, will also increase the water demands in future. To be more precise, based on Fig. 6, the water requirement of irrigated agriculture will increase to more than 1180 billion cubic meters (BCUM) in 2030 and more than 1300 BCUM in 2040. The water requirement of gardens, as the second land cover category with the highest water consumption, will increase to more than 175 BCUM in 2030 and about 270 BCUM in 2040. Furthermore, the water requirement of

Fig. 7 Water requirement of the sub-basin of West Azarbaijan Province for agriculture in the period of 2030–2040

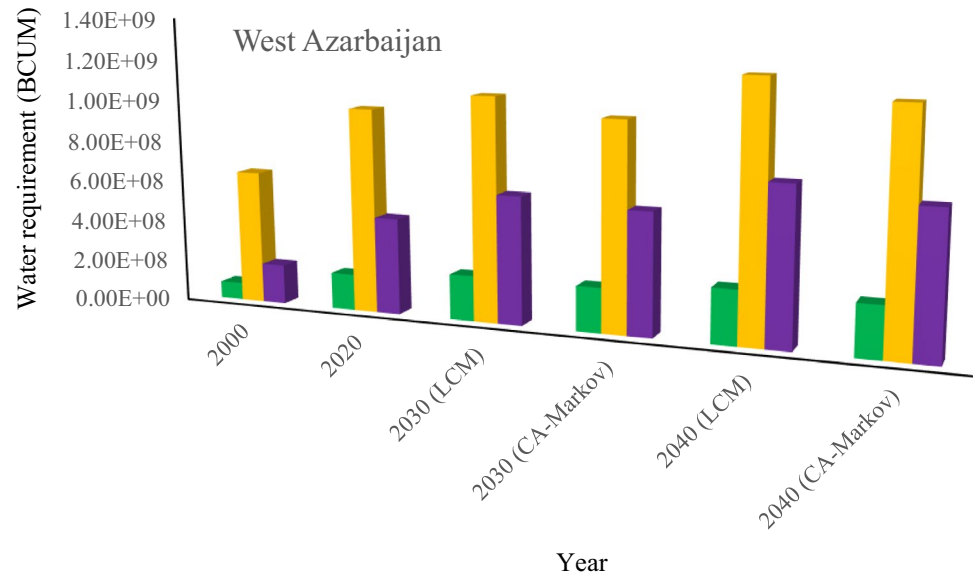
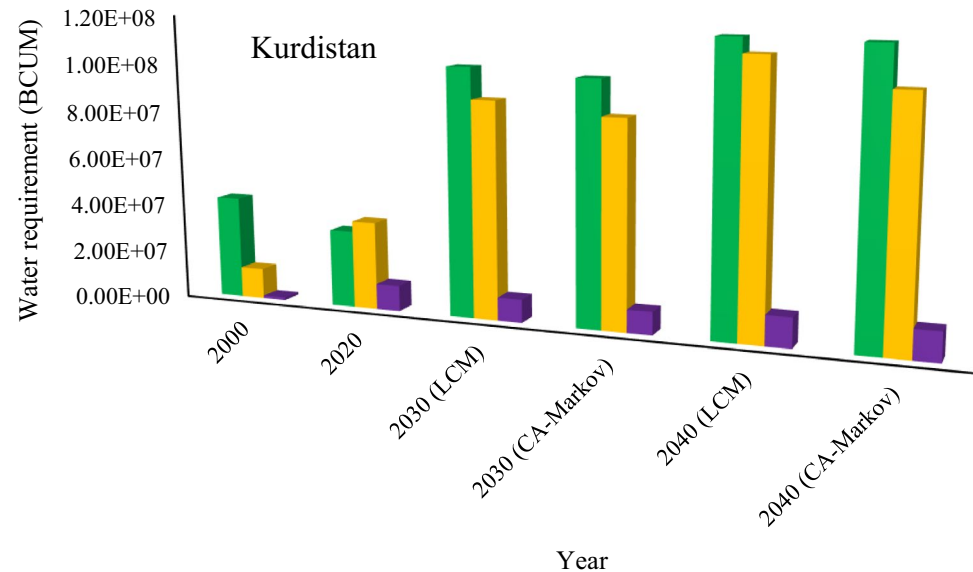


Fig. 8 Water requirement of the sub-basin of Kurdistan Province for agriculture in the period of 2030–2040

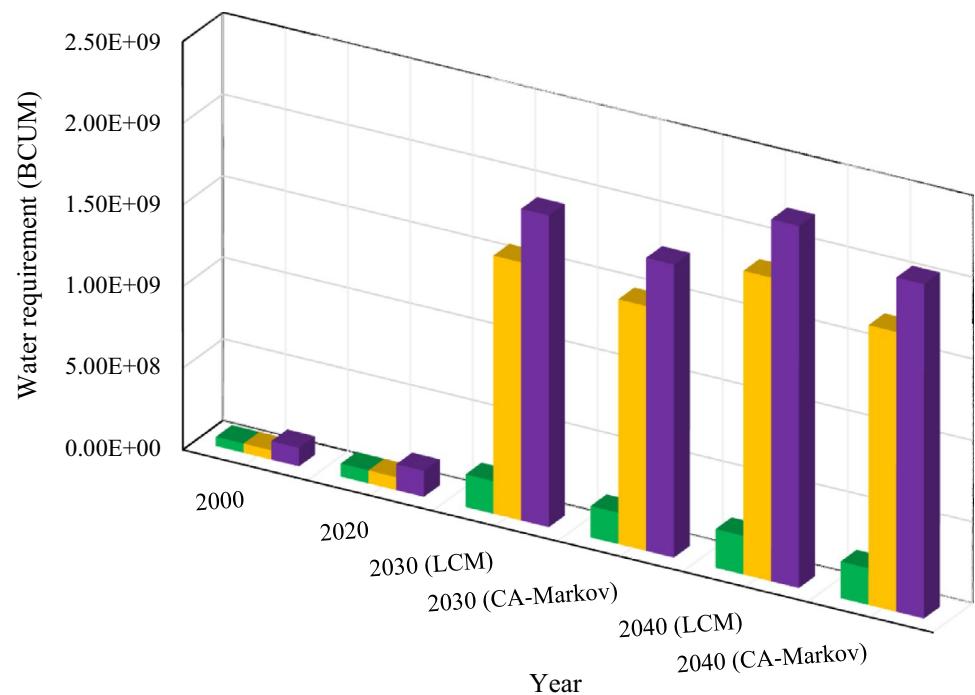


rain-fed agriculture will reach more than 140 BCUM in 2030 and more than 150 BCUM in 2040.

Figures 7 and 8 show that the water requirement of rain-fed agriculture in the sub-basin of West Azerbaijan and Kurdistan will increase to (218 and 100) BCUM and (150 and 115) BCUM in 2030 and 2040, respectively. The water requirement of gardens in the mentioned sub-basins will also increase to (600 and 95) BCUM, and (700 and 122) BCUM in 2020 and 2040, respectively. Finally, the water requirement of irrigated agriculture in these sub-basins will reach (1000 and 85) BCUM in 2030 and more than (1115 and 105) BCUM in 2040.

Figure 9 illustrates that the West Azerbaijan sub-basin will account for the largest share of future water consumption in the agricultural section. The findings show that the annual water requirement for agriculture will increase from 1850 BCUM in 2030 to more than 2100 BCUM in 2040. Analyzing the obtained results of the modeling process indicates a total increase of about 100% in the water requirement of agriculture in 30 years, so that this amount will increase from 1500 BCUM in 2000 to more than 3100 BCUM in 2030. Furthermore, this growth trend will reach more than 2.7 times by the year 2040, and the water requirement of agriculture in the Urmia Lake basin will reach more than 4100 BCUM.

Fig. 9 Changing trend of the water requirement of agriculture in the catchment area of the Urmia Lake during the period 2030–2040



Conclusion

The decrease in saline lakes, which consist of 44% of all available lake water, is a serious concern. In many parts of the world, lake drying is caused by water management failures. The Urmia Lake, the largest inland lake in Iran and the second-largest hyper-saline lake in the world, has undergone a dramatic decline (by about 8 m) in its water level since 1995. Problems associated with unbalanced agricultural development, particularly that of indiscriminate withdrawal of water resources, remain a pressing challenge for the Urmia Lake in the northwest of Iran. According to the presented statistics, the volume of renewable water resources in the catchment area of Urmia Lake was 7024 BCUM, and the volume of water consumption in different sections until 2013 was 4825 BCUM. However, changing land use and cultivation patterns from irrigated agriculture to horticulture had increased water consumption in this basin. In this study, the impacts of the agricultural land-use change in water requirements of crops in the Urmia Lake basin were identified and quantified. The results showed that the area covered by agricultural activities (rain-fed, irrigated agriculture, and gardens) has increased rapidly, so that the area covered by irrigated agriculture has increased from 0.028% of the total basin area in 2000 to more than 0.064% in 2030 and about 0.070% of the total basin area in 2040. The area covered by gardens will also increase from 0.007% of the total basin area in 2000 to more than 0.026% and 0.032% in 2030, and

2040, respectively. Finally, the area covered by rain-fed agriculture will reach more than 0.029% of the total area of the catchment area of the Urmia Lake, with an increase of about 0.011% compared to the base year 2000. The CA-Markov and LCM models simulation for the potential distribution of the LULC classes showed that the changes in the landscape that has experienced in the recent past are likely to continue. According to the outcomes of the NETWAT model, the water requirement of agriculture in the period of 40 years (2000 to 2040) has increased significantly from 1500 BCUM to more than 4500 BCUM. These results denote the high priority of establishing proper regulations and policies to restrict land-use changes in the Urmia Lake basin.

Funding No funding was received for conducting this study.

Availability of data and materials The data and materials that support the findings of this study are available on request from the corresponding author.

Declarations

Conflict of interests The authors declare that they have no competing interests.

Ethical approval Not applicable, because this article does not contain any studies with human or animal subjects.

Consent to participate Not applicable.

Consent for publication Not applicable.

References

- Abungba JA, Adjei KA, Gyamfi C, Odai SN, Pingale SM, Khare D (2022) Implications of Land Use/Land Cover changes and climate change on black volta basin future water resources in Ghana. *Sustainability* 14(19):12383. <https://doi.org/10.3390/su141912383>
- Ackom B, Olmedo MTC (2016) Scenario of land use and land cover change in the Gaza Strip using remote sensing and GIS models. *Arab J Geosci* 9:1–14. <https://doi.org/10.1007/s12517-015-2292-7>
- Calanca P (2007) Climate change and drought occurrence in the Alpine region: how severe are becoming the extremes? *Glob Planet Change* 57:151–160. <https://doi.org/10.1016/j.gloplacha.2006.11.001>
- Cawley GC, Talbot NL (2010) On over-fitting in model selection and subsequent selection bias in performance evaluation. *J Mach Learn Res* 11:2079–2107
- Cortes C, Vapnik V (1995) Support-vector networks. *Mach Learn* 20:273–297. <https://doi.org/10.1007/BF00994018>
- Dadhich PN, Hanaoka S (2010) Remote sensing, GIS and Markov's method for land use change detection and prediction of Jaipur district. *J Geomat* 4:9–15
- de Hipt FO, Diekkrüger B, Steup G, Yira Y, Hoffmann T, Rode M, Näschen K (2019) Modeling the effect of land use and climate change on water resources and soil erosion in a tropical West African catchment (Dano, Burkina Faso) using SHETRAN. *Sci Total Environ* 653:431–445. <https://doi.org/10.1016/j.scitotenv.2018.10.351>
- Eastman JR, Toledano J (2018) A short presentation of the Land Change Modeler (LCM). *Geomatic approaches for modeling land change scenarios*. Springer, Cham, pp 499–505
- Eastman JR (2006) *IDRISI andes guide to GIS and Image Processing*; Clark University: Worcester, MA USA, p 328
- Fauvel M, Chanussot J, Benediktsson JA (2009) Kernel principal component analysis for the classification of hyperspectral remote sensing data over urban areas. *EURASIP J Adv Signal Process*. <https://doi.org/10.1155/2009/783194>
- Fu F, Deng S, Wu D, Liu W, Bai Z (2022) Research on the spatiotemporal evolution of land use landscape pattern in a county area based on CA-Markov model. *Sustain Cities Soc* 80:103760. <https://doi.org/10.1016/j.scs.2022.103760>
- Goodarzi MR, Mohtar RH, Piryaei R, Fatehifar A, Niazkari M (2022) Urban WEF nexus: an approach for the use of inland resources under climate change. *Hydrology* 9(10):176. <https://doi.org/10.3390/hydrology9100176>
- Grechi RC, Gwyn QHJ, Béné GB, Formaggio AR, Fahl FC (2014) Land use and land cover changes in the Brazilian Cerrado: a multidisciplinary approach to assess the impacts of agricultural expansion. *Appl Geogr* 55:300–312. <https://doi.org/10.1016/j.apgeog.2014.09.014>
- Guan D, Li H, Inohae T, Su W, Nagaie T, Hokao K (2011a) Modeling urban land use change by the integration of cellular automaton and Markov model. *Ecol Modell* 222:3761–3772. <https://doi.org/10.1016/j.ecolmodel.2011.09.009>
- Guan D, Li H, Inohae T, Su W, Nagaie T, Hokao K (2011b) Modeling urban land use change by the integration of cellular automaton and Markov model. *Ecol Model* 222(20–22):3761–3772. <https://doi.org/10.1016/j.ecolmodel.2011.09.009>
- Hasan S, Shi W, Zhu X, Abbas S, Khan HUA (2020) Future simulation of land use changes in rapidly urbanizing South China based on land change modeler and remote sensing data. *Sustainability* 12:4350. <https://doi.org/10.3390/su12114350>
- Hosseini Baghanam A, Seifi AJ, Sheikhabaei A, Hassanzadeh Y, Besharat M, Asadi E (2022) Policy-making toward integrated water resources management of Zarrine River basin via system dynamics approach under climate change impact. *Sustainability* 14(6):3376. <https://doi.org/10.3390/su14063376>
- Hussien K, Kebede A, Mekuriaw A, Asfaw Beza S, Haile Erena S (2022) Modelling spatiotemporal trends of land use land cover dynamics in the Abbay River Basin. *Ethiopia Model Earth Syst Environ*. <https://doi.org/10.1007/s40808-022-01487-3>
- Idrissou M, Diekkrüger B, Tischbein B, Op de Hipt F, Näschen K, Poméon T, Ibrahim B (2022) Modeling the Impact of climate and Land Use/Land Cover change on water availability in an inland valley catchment in Burkina Faso. *Hydrology* 9(1):12. <https://doi.org/10.3390/hydrology9010012>
- Kumar N, Singh SK, Singh VG, Dzwauro B (2018) Investigation of impacts of land use/land cover change on water availability of Tons River Basin, Madhya Pradesh India. *Model Earth Syst Environ* 4(1):295–310. <https://doi.org/10.1007/s40808-018-0425-1>
- Kumar S, Radhakrishnan N, Mathew S (2014) Land use change modelling using a Markov model and remote sensing. *Geomat Nat Hazards Risk* 5:145–156. <https://doi.org/10.1080/19475705.2013.795502>
- Li Z, Liu WZ, Zhang XC, Zheng FL (2009) Impacts of land use change and climate variability on hydrology in an agricultural catchment on the Loess Plateau of China. *J Hydrol* 377:35–42. <https://doi.org/10.1016/j.jhydrol.2009.08.007>
- Ma C, Zhang GY, Zhang XC, Zhao YJ, Li HY (2012) Application of markov model in wetland change dynamics in tianjin coastal area, China. *Procedia Environ Sci* 13:252–262. <https://doi.org/10.1016/j.proenv.2012.01.024>
- Mansour S, Al-Belushi M, Al-Awadhi T (2020) Monitoring land use and land cover changes in the mountainous cities of Oman using GIS and CA-Markov modelling techniques. *Land Use Policy* 91:104414. <https://doi.org/10.1016/j.landusepol.2019.104414>
- Maviza A, Ahmed F (2020) Analysis of past and future multi-temporal land use and land cover changes in the semi-arid Upper-Mzingwane sub-catchment in the Matabeleland south province of Zimbabwe. *Int J Remote Sens* 41(14):5206–5227. <https://doi.org/10.1080/01431161.2020.1731001>
- Memarian H, Balasundram SK, Talib JB, Sung CTB, Sood AM, Abbaspour K (2012) Validation of CA-Markov for simulation of land use and cover change in the Langat Basin, Malaysia. <https://doi.org/10.4236/jgis.2012.46059>
- M Mishra, KK Mishra, AP Subudhi, M Phil, O Cuttack (2011) Urban sprawl mapping and land use change analysis using remote sensing and GIS. In *Geospatial World Forum*.
- Montalván-Burbano N, Velastegui-Montoya A, Gurumendi-Noriega M, Morante-Carballo F, Adami M (2021) Worldwide research on land use and land cover in the Amazon region. *Sustainability* 13(11):6039. <https://doi.org/10.3390/su13116039>
- Mosammam HM, Nia JT, Khani H, Teymouri A, Kazemi M (2017) Monitoring land use change and measuring urban sprawl based on its spatial forms: the case of Qom city. *Egyptian J Remote Sensing Space Sci* 20(1):103–116. <https://doi.org/10.1016/j.ejrs.2016.08.002>
- Mubea KW, Ngigi TG, Mundia CN (2011) Assessing application of Markov chain analysis in predicting land cover change: a case study of Nakuru municipality. *J Agric Sci Technol* 12(2):126–144
- Ni X, Parajuli PB, Ouyang Y, Dash P, Siegert C (2021) Assessing land use change impact on stream discharge and stream water quality in an agricultural watershed. *CATENA* 198:105055. <https://doi.org/10.1016/j.catena.2020.105055>
- Nouri J, Gharagozlou A, Arjmandi R, Faryadi S, Adl M (2014) Predicting urban land use changes using a CA-Markov model. *Arab J Sci Eng* 39:5565–5573. <https://doi.org/10.1007/s13369-014-1119-2>
- Nyatuame M, Amekudzi LK, Agodzo SK (2020) Assessing the land use/land cover and climate change impact on water balance on Tordzie watershed. *Remote Sensing Appl Soc Environ* 20:100381. <https://doi.org/10.1016/j.rsase.2020.100381>

- Ougahi JH, Karim S, Mahmood SA (2022) Application of the SWAT model to assess climate and land use/cover change impacts on water balance components of the Kabul River Basin, Afghanistan. *J Water Climate Change*. 13(11):3977. <https://doi.org/10.2166/wcc.2022.261>
- Overmars KD, De Koning GHJ, Veldkamp A (2003) Spatial autocorrelation in multi-scale land use models. *Ecol Modell* 164:257–270. [https://doi.org/10.1016/S0304-3800\(03\)00070-X](https://doi.org/10.1016/S0304-3800(03)00070-X)
- Pontius GR, Malanson J (2005) Comparison of the structure and accuracy of two land change models. *Int J Geogr Inf Sci* 19:243–265. <https://doi.org/10.1080/13658810410001713434>
- Prakasam C (2010) Land use and land cover change detection through remote sensing approach: a case study of Kodaikanal taluk, Tamil nadu. *Intern J Geomat Geosci* 1(2):150
- Qacami M, Khattabi A, Lahssini S, Rifai N, Meliho M (2022) Land-cover/land-use change dynamics modeling based on land change modeler. *Ann Reg Sci*. <https://doi.org/10.1007/s00168-022-01169-z>
- Reis S (2008) Analyzing land use/land cover changes using remote sensing and GIS in Rize. *North-East Turkey Sensors* 8(10):6188–6202. <https://doi.org/10.3390/s8106188>
- Sahoo S, Dhar A, Debsarkar A, Kar A (2018) Impact of water demand on hydrological regime under climate and LULC change scenarios. *Environment Earth Sci* 77(9):1–19. <https://doi.org/10.1007/s12665-018-7531-2>
- Samal DR, Gedam S (2021) Assessing the impacts of land use and land cover change on water resources in the Upper Bhima river basin India. *Environment Challeng* 5:100251. <https://doi.org/10.1016/j.envc.2021.100251>
- Sang L, Zhang C, Yang J, Zhu D, Yun W (2011) Simulation of land use spatial pattern of towns and villages based on CA–Markov model. *Math Comput Model* 54(3–4):938–943. <https://doi.org/10.1016/j.mcm.2010.11.019>
- Schilling KE, Jha MK, Zhang YK, Gassman PW, Wolter CF (2008) Impact of land use and land cover change on the water balance of a large agricultural watershed: Historical effects and future directions. *Water Res Res*. <https://doi.org/10.1029/2007WR006644>
- Shooshtarian MR, Dehghani M, Margherita F, Gea OC, Morteza-zadeh S (2018) Land use change and conversion effects on ground water quality trends: an integration of land change modeler in GIS and a new Ground Water Quality Index developed by fuzzy multi-criteria group decision-making models. *Food Chem Toxicol* 114:204–214. <https://doi.org/10.1016/j.fct.2018.02.025>
- Sibanda S, Ahmed F (2021) Modelling historic and future land use/land cover changes and their impact on wetland area in Shashe sub-catchment, Zimbabwe. *Model Earth Syst Environ* 7:57–70. <https://doi.org/10.1007/s40808-020-00963-y>
- Singh SK, Srivastava PK, Gupta M, Thakur JK, Mukherjee S (2014) Appraisal of land use/land cover of mangrove forest ecosystem using support vector machine. *Environ Earth Sci* 71:2245–2255. <https://doi.org/10.1007/s12665-013-2628-0>
- Tariq A, Yan J, Mumtaz F (2022) Land change modeler and CA–Markov chain analysis for land use land cover change using satellite data of Peshawar. *Pakistan Phys Chem Earth*. <https://doi.org/10.1016/j.pce.2022.103286>
- Veldkamp A, Lambin EF (2001) Predicting land-use change. *Agric Ecosyst Environ* 85:1–6. [https://doi.org/10.1016/S0167-8809\(01\)00199-2](https://doi.org/10.1016/S0167-8809(01)00199-2)
- Wang SW, Gebru BM, Lamchin M, Kayastha RB, Lee WK (2020) Land use and land cover change detection and prediction in the Kathmandu district of Nepal using remote sensing and GIS. *Sustainability* 12:3925. <https://doi.org/10.3390/su12093925>
- Weng Q (2002) Land use change analysis in the Zhujiang Delta of China using satellite remote sensing, GIS and stochastic modeling. *J Environ Manage* 64:273–284. <https://doi.org/10.1006/jema.2001.0509>
- Weslati O, Bouaziz S, Sarbeji MM (2022) Modelling and assessing the spatiotemporal changes to future land use change scenarios using remote sensing and CA-markov model in the mellegue catchment. *J Indian Soc Remote Sens*. <https://doi.org/10.1007/s12524-022-01618-4>
- Wu L, Shi P, Gao H (2010) State estimation and sliding-mode control of Markovian jump singular systems. *IEEE Trans Autom Control* 55(5):1213–1219. <https://doi.org/10.1109/TAC.2010.2042234>
- Yang Q, Li X, Shi X (2008) Cellular automata for simulating land use changes based on support vector machines. *Comput Geosci* 34:592–602. <https://doi.org/10.1016/j.cageo.2007.08.003>
- Yang X, Zheng XQ, Lv LN (2012) A spatiotemporal model of land use change based on ant colony optimization, Markov chain and cellular automata. *Ecol Model* 233:11–19. <https://doi.org/10.1016/j.ecolmodel.2012.03.011>
- Zhang R, Tang C, Ma S, Yuan H, Gao L, Fan W (2011) Using Markov chains to analyze changes in wetland trends in arid Yinchuan Plain, China. *Math Comput Model* 54:924–930. <https://doi.org/10.1016/j.mcm.2010.11.017>

Publisher's Note Springer Nature remains neutral with regard to jurisdictional claims in published maps and institutional affiliations.

Springer Nature or its licensor (e.g. a society or other partner) holds exclusive rights to this article under a publishing agreement with the author(s) or other rightsholder(s); author self-archiving of the accepted manuscript version of this article is solely governed by the terms of such publishing agreement and applicable law.